

## STAR results on femtoscopy at the BES program

---

**Hanna Paulina Zbroszczyk for the STAR Collaboration<sup>\*†</sup>**

*Warsaw University of Technology*

*Faculty of Physics*

*Koszykowa 75*

*00-662 Warsaw, POLAND*

*E-mail: [hanna.zbroszczyk@pw.edu.pl](mailto:hanna.zbroszczyk@pw.edu.pl)*

Geometry and dynamics of the particle-emitting source in heavy-ion collisions can be inferred via the femtoscopy method. Two-particle correlations at small relative momentum exploit Quantum Statistics (QS) and the Final State Interactions (FSI), which allow one to study the space-time characteristics of the source of the order of  $10^{-15}$  m and  $10^{-23}$  s. The RHIC Beam Energy Scan (BES) program covers a significant part of the QCD Phase Diagram using Au nuclei collisions for several beam energies from 3.0 to 200 GeV, where the baryon-rich region is studied via femtoscopy. Together with meson ones, baryon measurements provide complementary information about the source created in the final states of interactions. The results of non-identical particles enable studies of space-time asymmetries in the emission process. Besides, femtoscopy enables the investigation of FSI between hadrons. The femtoscopic measurements of various particle combinations for different collision energies and centralities will be shown in these proceedings.

*CPOD 2021 - the International conference on Critical Point and Onset of Deconfinement*

*15 - 19 March 2021*

*Zoom*

---

<sup>\*</sup>Speaker.

<sup>†</sup>

## 1. Introduction

Solenoidal Tracker At RHIC (STAR) is an experiment realized at Relativistic Heavy Ion Collider (RHIC) at Brookhaven National Laboratory (BNL), Upton. The STAR experiment's primary goal is to study the properties of matter created under extreme conditions (such as pressure, density) and learn about interactions between hadrons. For more than 20 years, STAR has been collecting data from various collisions of different ions at different energies:  $\sqrt{s_{NN}} = 7.7, 11.5, 14.5, 19.6, 27, 39, 54.4, 62.4, 130,$  and  $200$  GeV in the collider mode, and recently in the fixed target too, where the data has been available from  $\sqrt{s_{NN}} = 4.5$  GeV. The highest collision energy of Au nuclei is  $\sqrt{s_{NN}} = 200$  GeV, and it enables the measurement of hot and dense matter after QGP formation. The Beam Energy Scan (BES) program [1, 2] which includes colliding energies below  $\sqrt{s_{NN}} = 62.4$  GeV, is mainly focused on the exploration of the QCD phase transition between Quark-Gluon Plasma (QGP) and hadron gas and also to search for the Critical Point (CP) between first-order phase-transition and cross-over transition described by Quantum Chromodynamics (QCD).

## 2. Details of analysis

In order to define a femtoscopic correlation function [3, 4], in the case of identical particle combinations a Lonitudinally Co-Moving System (LCMS) is used which is defined as  $p_{L,1} + p_{L,2} = 0$ .  $p_{L,1}$  and  $p_{L,2}$  are longitudinal components of momentum for single particles. Using LCMS system the correlation function is defined using  $Q_{\text{inv}} = \sqrt{(p_1 - p_2)^2 - (E_1 - E_2)^2}$  variable. In the case of nonidentical particle combinations, Pair Rest Frame (PRF) reference is used which defines  $k^* = p_1 = -p_2$  variable. The PRF reference can be also used for identical pairs of particles and then  $Q_{\text{inv}} = 2k^*$ .

The definition of the correlation functions is as follows:  $C(k^*) = \frac{A(k^*)}{B(k^*)}$  or  $C(Q_{\text{inv}}) = \frac{A(Q_{\text{inv}})}{B(Q_{\text{inv}})}$ . Correlated pairs of particles (from the same event) enter the numerator  $A(k^*)$  or  $A(Q_{\text{inv}})$  and uncorrelated pairs of particles (from different events) enter the denominator  $B(k^*)$  or  $B(Q_{\text{inv}})$  of the correlation function. All particles are measured and identified with two detectors: the Time Projection Chamber (TPC) and the Time of Flight (TOF).

The centrality selection is determined based on the uncorrected primary charged-particle multiplicity measured in the pseudorapidity region ( $|\eta| < 0.5$ ) as given by the TPC detector. The fraction of this multiplicity distribution defines the centrality classes. The centrality class defined as 0 – 10% corresponds to the most central collisions calculated in the amount of up to 10% of the total hadronic cross-section of the collision, while the 70 – 80% bin is related to the most peripheral collisions. All particles are identified using the energy loss in the TPC detector ( $dE/dx$ ). In the case of identical pion femtoscopy, following centrality bins are used: 0-5%, 5-10%, 10-15%, 15-20%, 20-25%, 25-30%. In case proton or nonidentical particle correlations (within the centrality up to 80%) minimum Bias Au+Au collisions are divided into three centrality classes: central (0-10%), mid-central (10-30%), and peripheral (30-80%).

Pions are chosen in the transverse momentum range:  $0.2 < p_T < 2.0$  GeV/c and kaons within  $0.2 < p_T < 2.0$  GeV/c. Protons and antiprotons are chosen in the transverse momentum range:  $0.4 < p_T < 2.5$  GeV/c. All particles are taken from the rapidity interval  $|Y| < 0.5$  for the collider mode and  $-0.5 < Y < 1.5$  for the fixed-target mode. Each track is extrapolated to the primary

42 vertex. If the shortest distance between the track and the vertex exceeds 1 cm, the track is excluded  
 43 from the analysis chain. It removes a significant fraction of non-primary track candidates. Infor-  
 44 mation derived from the TOF detector allows one to estimate the mass of the particle. We require  
 45 the mass square of pions to be between 0.01 and 0.03  $(\text{GeV}/c^2)^2$ , of kaons within 0.21 and 0.28  
 46  $(\text{GeV}/c^2)^2$  and of protons to be between 0.76 and 1.03  $(\text{GeV}/c^2)^2$ . The particle purity is not taken  
 47 into account as it is estimated as almost 100%. The effects of track-splitting and track-merging are  
 48 also taken into account.

### 49 **3. Geometry of the collision**

50       As a result of the heavy-ion collision, a hot and dense system produces different types of  
 51 particles. Using the femtoscopy method, it is possible to learn about the source's geometrical and  
 52 dynamical properties. Geometrical parameters are related to sizes and dynamical ones to space-  
 53 time emission sequences of particles of different species. Femtoscopy enables one to study of space  
 54 characteristics of particle pairs emitted from the source. Thus, it is impossible to explore the whole  
 55 source's information but rather to its part, correlated pairs of emitting particles. It explains why  
 56 source sizes extracted from various studies are different depending on the considered system. So  
 57 the geometry of heavy-ion collision can be studied via femtoscopic parameters describing source  
 58 sizes of emission areas.

#### 59 **3.1 Results for pions femtoscopy at Au + Au collisions for BES program**

60       Identical pion correlations are performed in three-dimensional space where *long* component is  
 61 determined by the beam axis, *out* component by the pair transverse momentum, and *side* compo-  
 62 nent is perpendicular to their both. Figure 1 shows results from identical pion femtoscopy measured  
 63 in the BES program. Upper plot shows  $R_{out}^2 - R_{side}^2$  measured as a function of collision energy. There  
 64 is visible and characteristic peak around  $\sqrt{s_{NN}} \simeq 20$  GeV indicating a possible region of the phase  
 65 transition. Bottom plot presents  $\frac{R_{out}}{R_{side}}(\sqrt{s_{NN}})$  indicating a similar trend around the same collision  
 66 energy.

67       There is a known trend for higher collision energies that the source is more prolonged in the  
 68 transverse direction than in the longitudinal one ( $R_{long} > R_{side}$ ), and for lower collision energies,  
 69 the trend is opposite. Figure 2 shows the relation between  $R_{side}$  and  $R_{long}$  for different experimental  
 70 facilities indicating that at  $\sqrt{s_{NN}} = 4.5$  GeV the measured source is round-shaped.

#### 71 **3.2 Results for protons femtoscopy at Au + Au collisions for BES program**

72       Figure 3 shows results of proton-proton correlation functions for  $\sqrt{s_{NN}} = 39$  GeV for three  
 73 different centralities. Figure 4 presents the results for proton-antiproton correlation functions for  
 74 the same centrality classes. Centrality dependence is seen. Presented results indicate that source  
 75 size strongly depends on collision centrality (in the case of more central collisions, more immense  
 76 source is produced indicated by a weaker correlation signal, while in the case of more peripheral  
 77 collisions, a smaller source and stronger correlation are measured). The correlation effect (width  
 78 and magnitude of the correlation function) depends inversely proportional to the source size. Radii  
 79 of the source also depend on collision energy. For higher collision energy more prominent source  
 80 and a weaker correlation is registered.

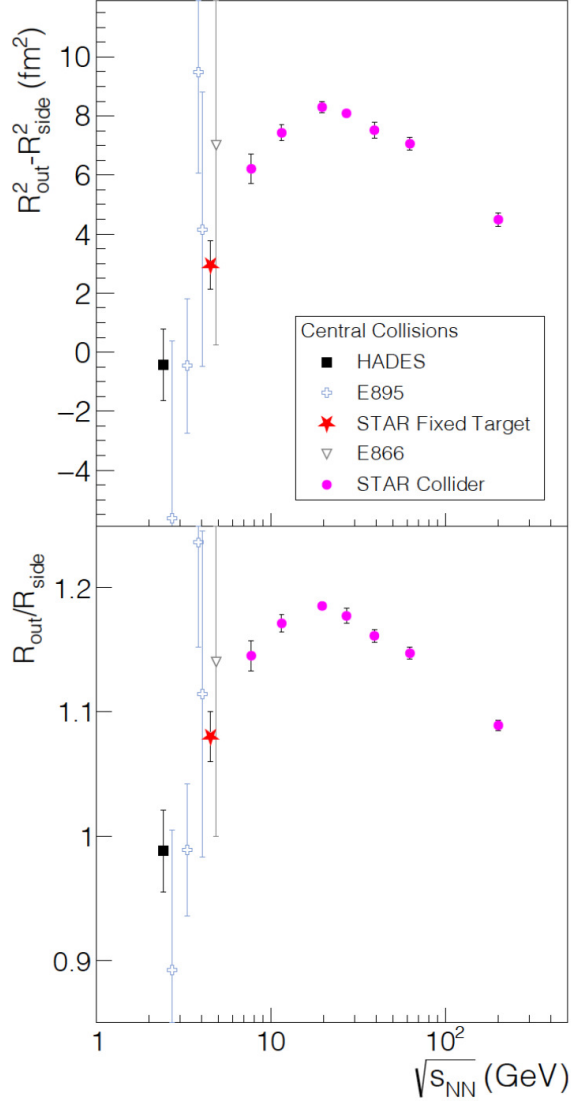


**Figure 1:**  $R_{out}^2 - R_{side}^2$  (top) and  $\frac{R_{out}}{R_{side}}$  measured as a function of  $\sqrt{s_{NN}}$  for identical pion interferometry results from the BES program [5]

#### 81 4. Dynamics of the collision

82 The dynamics of the collision can be studied using femtoscopic methods using only non-  
 83 identical particle combinations. It is possible to study the emission sequence in the case of distin-  
 84 guishable particles. Collision dynamics can be related to space and time aspects. The femtoscopy  
 85 method is sensitive to the emission asymmetries related to the spatial shifts (particles of different  
 86 types statistically emitted from different areas of the emission source) and the time intervals be-  
 87 tween the two different particles' emissions. However, it is impossible to distinguish whether space  
 88 and/or time asymmetry is deduced. In the case of such studies, the measured correlation function  
 89 is determined using Spherical Harmonics decompositions [6]. Thus, it is possible to study two

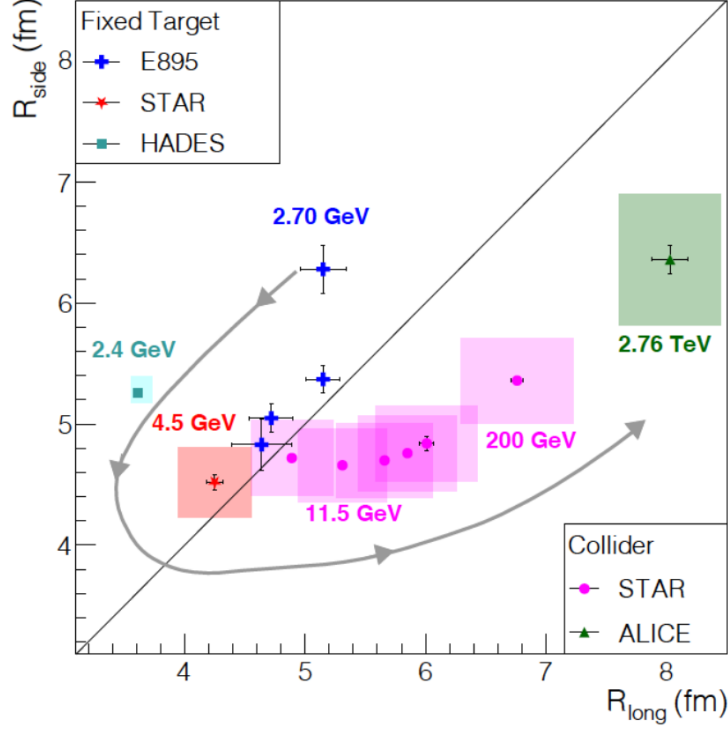


**Figure 2:**  $R_{side}$  and  $R_{long}$  measured for different collision energies for identical pion interferometry [5]

90 components:  $C_0^0(k^*)$ , which is consistent with the one-dimensional correlation function  $C(k^*)$ , and  
 91  $C_1^1(k^*)$ , which is sensitive to the possible asymmetries in the emission process. Figure 5 shows  
 92 correlation functions ( $C_1^1$  components) for pion-kaon systems for various collision centralities for  
 93 collision energy  $\sqrt{s_{NN}} = 39$  GeV. All  $C_1^1$  functions are different from zero value for small  $k^*$  in-  
 94 tervals. It confirms emission asymmetries, proving that lighter particles (pions) are statistically  
 95 emitted closer to the system's center and/or earlier than heavier particles (kaons). Such asymme-  
 96 tries are caused by the flow phenomenon, which affects particles differently with different masses.

## 97 5. Summary

98 This paper presents results describing the geometrical and dynamical properties of the source  
 99 produced during heavy-ion collisions. In the context of geometrical properties, results of the iden-  
 100 tical pions, proton-proton, antiproton-antiproton, and proton-antiproton femtoscopy for Au + Au  
 101 collisions at the BES program at STAR are discussed. For identical pion interferometry, the re-  
 102 lation between source sizes in *out* and *side* directions are discussed as a possible signature of the  
 103 phase transition. From studies performed in the BES program, invariant source sizes are extracted  
 104 for proton-proton, proton-antiproton, and antiproton-antiproton pairs. The effect of residual corre-  
 105 lations (including products of weak decays) is not considered, and it would be reflected in discrep-  
 106 ancies between the source sizes estimated for identical and non-identical combinations of protons  
 107 and antiprotons. Presented results underline the significance of change the source sizes with dif-

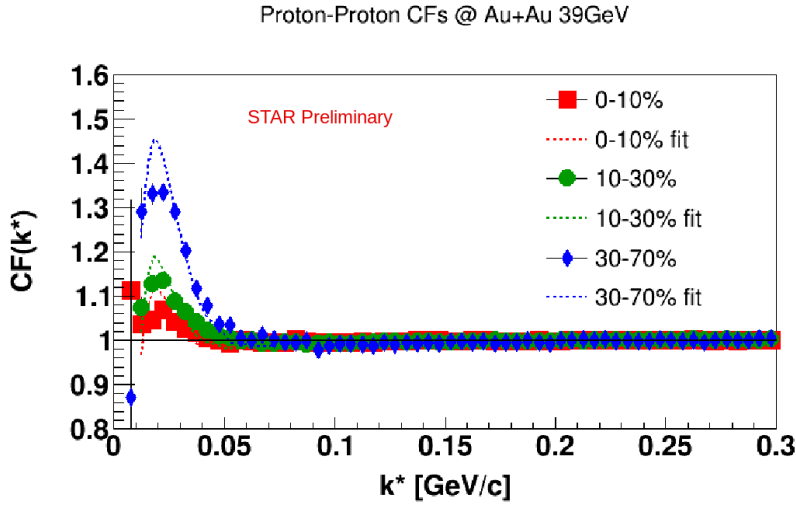


Figure 3: Proton-proton correlation functions for different centrality classes for  $\sqrt{s_{NN}} = 39$  GeV [7, 8]

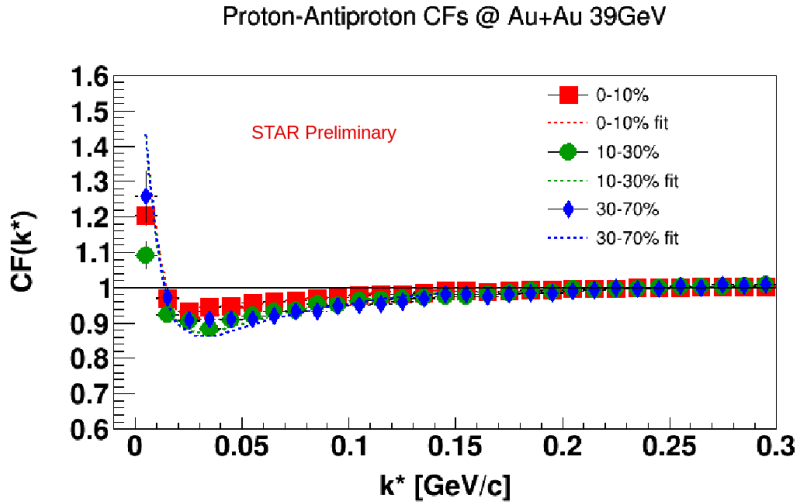
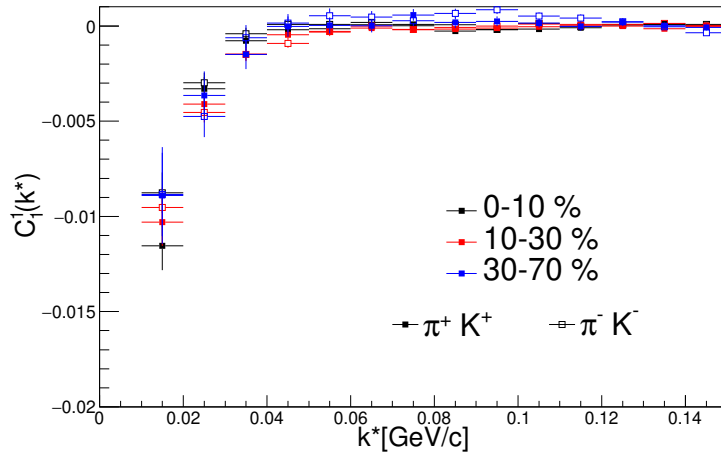


Figure 4: Proton-antiproton correlation functions for different centrality classes for  $\sqrt{s_{NN}} = 39$  GeV [7, 8]

108 ferent collision centrality or collision energy. In the context of geometrical properties, results of  
 109 pion-kaon correlations are discussed. They prove that emission differences of distinguishable par-  
 110 ticles can originate in both: spatial and time components. Both of them are the result of different  
 111 emission properties for particles with different masses. Shown results confirm that lighter particles  
 112 are, on average, emitted closer to the system's center and /or earlier than heavier ones.

### 113 Acknowledgments

114 This work was supported by the Grant of National Science Centre, Poland, No: 2020/38/E/ST2/00019.  
 115 Studies were funded by IDUB-POB-FWEiTE-1 project granted by Warsaw University of Technol-  
 116 ogy under the program Excellence Initiative: Research University (ID-UB).



**Figure 5:** Pion-kaon correlation functions for different centrality classes for  $\sqrt{s_{NN}} = 39$  GeV [8]

117 **References**

118 [1] G. Odyniec *et al.*, J. Phys. **G37**, 094028 (2010)  
 119 [2] M.M.Aggarwal *et al.*, arXiv:1007.2613v1  
 120 [3] V.G. Grishin, G.I. Kopylov, M.I. Podgoretskii, Sov. J. Nucl. Phys. **13** (1971) 638  
 121 [4] R. Lednicky, V. L. Lyuboshitz, Sov. Journ. Nucl. Phys. **35** (1982) 770  
 122 [5] J. Adam, H. Zbroszczyk *et al.*, Phys. Rev. C **103** (2021) 034908  
 123 [6] P. Danielewicz and S.Pratt. Phys. Lett. **B618** (2005) 60  
 124 [7] H. Zbroszczyk *et al.*, Proceedings of Workshop on Particle Correlations and Femtoscopy, Acta  
 125 Phys.Polon.Supp. **13** (2020) 619  
 126 [8] S. Siejka *et al.*, Nucl.Phys. **A982** (2019) 359-362